XLI CILAMCE
XLI Ibero-Latin American Congress on Computational Methods in Engineering
16-19 November, 2020 FOZ DO IGUAÇU PARANÁ - BRAZIL

Constitutive modeling of viscoelastic materials: A quantitative comparison between classic and fractional models

M. E. W. Costa[1], J.-M. C. Farias[1], L. B. P. de Faria[1], E. A. Fancello[1]

[1]*Dept. of Mechanical Engineering, Federal University of Santa Catarina*
Florianópolis, 88040-900, SC, Brazil
eduardo.fancello@ufsc.br

Abstract. Thermoplastic polymers are widely used in biomedical applications, such as knee and hip prosthetics. The development of optimized orthopedic implants is strongly related to the performance of experimental tests and computer simulations that approximate the behavior *in situ* of the material used. The literature indicates the possibility of applying fractional viscoelastic constitutive models as an alternative to the classical integer order models. However, it is not common to compare quantitatively the results obtained using both approaches. Therefore, the predictive capabilities of some fractional and classical viscoelastic models with infinitesimal and finite kinematics are compared in this work. The study is conducted using cyclical and creep-recovery experimental tests at two strain and stress rates. First we present the individual fittings of the cyclical and creep-recovery experimental data. Then, these tests are fitted simultaneously. The parameter fitting is made using a hybrid optimization procedure, using a heuristic method for global search and another based on gradients for local search. In the context of the experimental conditions evaluated, the results indicated that the use of the fractional models tested did not result in a significant improvement when the assessment are made using individual experimental data. On the other hand, for the the simultaneously parameter fitting, the fractional models showed a slight improvement. However, none of the models used was able to represent satisfactorily the cyclic and creep-recovery data used, this fact may be related to the presence of nonlinear phenomena not taken into account in the present work.

Keywords: Fractional Viscoelasticity, Constitutive modelling, Creep, Cyclic

1 Introduction

The classic constitutive modeling of viscoelastic materials is usually performed by means of phenomenological models. In this approach, the representation of the material behavior is obtained by elements that separately describe the elastic and the viscous behavior.

These elastic and viscous elements can be further combined in many different ways resulting in different models. Some of them are the well known Kelvin and Maxwell models, or a combination of these, yielding, for example, their generalized versions, as presented in Ward and Sweeney [1]. If one is to adopt the classical linear viscoelasticity theory to derive the constitutive laws, linear differential equations are obtained with derivatives that are known to have integer order. These classic viscoelastic approaches are also known to be sensitive to the entire past strain history of the material. However, due to the mathematical properties of them, when dealing with the incremental constitutive update algorithms, the dependence on the entire strain history may be reduced to account for only the two most recent states. This allows for an efficient computational implementation.

This intrinsic association with the past strain history and with linear differential equations automatically brought attention to the use of fractional derivatives. Interestingly, the concept of fractional derivatives embeds the entire history of the variable being differentiated within its own definition. Thus, it seems appropriate that this concept would naturally fit the modeling of viscoelastic materials as well, extending the order of the differential operators to fractional ones.

In contrast to its integer version, the fractional derivative is not uniquely determined, in the sense that there is a large number of definitions available in the literature. These alternative definitions may be specialized or better suited for different areas of interest. Formulations in the sense of Caputo, Riemann-Liouville (R.L.), and Grünwald-Letnikov (G.L.) are widely used.

Typically, two approaches are followed when dealing with fractional viscoelasticity. On the one hand, some authors analyze the fractional model entirely in the frequency domain. This approach is well suited when DMA tests are available and the storage and loss moduli are sought. For example, Xu et al. [2], used fractional models to analyze vibrations in beams in the frequency domain. Recently, Amabili et al. [3] compared the predictive capability of integer and fractional models with finite kinematics in fitting human aortas, also in frequency domain. On the other hand, fractional models can also be formulated in the time domain. This approach leads to differential equations with differential operators that are fractional. As a consequence of that, the incremental constitutive update algorithm must account for the entire past history of the variable being differentiated. This is the approach followed herein.

Although other works make the comparison in the time domain, to our knowledge, this approach is still scarce and the comparison is usually made using only one strain or stress rate per parameter fitting procedure, such as Meng et al. [4]. One can also cite the work made by Xiao et al. [5], where the authors carry out comparison in several load conditios, however, experimental results of real materials were not used. This work aims at contributing to this point. We investigate how fractional viscoelasticity aids at increasing the predictive capability when assessing two creep-recovery and two cyclic experiments simultaneously, both in the time domain, for a polymer widely used in biomedical applications. To avoid local minima, we adopted a hybrid procedure for fitting these models. First, the Particle Swarm Optimization method (PSO) is used for a global prospection of the parameter space, followed by a gradient-based method for a local parameter refinement.

2 Constitutive models

The models presented are formulated in terms of deviatoric and volumetric parts associated with each viscoelastic branch. This approach follows that presented by Adolfsson and Enelund [6] in his fractional model with finite kinematics. The volumetric part is assumed to be purely elastic. Therefore, the evolution of internal variables is given only by the deviatoric part (Adolfsson and Enelund [6], Khajehsaeid [7], Simo and Hughes [8]).

We should make an important observation about the Poisson's ratio. This ratio in viscoelastic materials can be a function of time (or frequency), as presented by Tschoegl et al. [9] for classic viscoelasticity. However, to consider this phenomenon, the strain in transverse direction should also be measured, or performed tests in pure hydrostatic and deviatoric conditions. Since no transverse strain data is available, we use the initial Poisson elastic ratio. Therefore, the bulk parameter, K_∞, is obtained from eq. (1), where G_∞ and G_i are deviatoric parameters. In addition, a Poisson's ratio, $\nu_0 = 0.46$, was considered.

$$\mathrm{K}_\infty = \frac{2(1+\nu_0)\mathrm{G}_0}{3(1-2\nu_0)}, \tag{1}$$

$$\mathrm{G}_0 = \mathrm{G}_\infty + \sum_{i=1}^{k} \mathrm{G}_i. \tag{2}$$

In the previous equations, "k" represents the number of Maxwell devices in parallel. The total stress, $\boldsymbol{\sigma}(t)$, can be obtained by the difference between the elastic and viscoelastic stress, according to the eq. (3). Where $\boldsymbol{\varepsilon}$, $\boldsymbol{e}$, Ψ and $\mathbf{Q}_i$, correspond, respectively, to the infinitesimal strain tensor and its deviatoric part, the Helmholtz free energy function and the internal variable tensor of each viscoelastic branch. The evolution of the internal variables $\mathbf{Q}_i$ is given by the integer order differential equation presented in the eq. (4), where τ_i is the viscoelastic relaxation time of each Maxwell's device. The dev term designates the spatial deviatoric operator.

$$\boldsymbol{\sigma}(t) = \frac{\partial \Psi_\infty(\boldsymbol{\varepsilon})}{\partial \boldsymbol{\varepsilon}} + \sum_{i=1}^{k} \frac{\partial \Psi_i(\mathbf{e})}{\partial \boldsymbol{\varepsilon}} - \sum_{i=1}^{k} \mathbf{Q}_i, \tag{3}$$

$$\frac{d\mathbf{Q}_i}{dt} + \frac{\mathbf{Q}_i}{\tau_i} = \frac{1}{\tau_i}\mathrm{dev}\left[\frac{\partial \Psi_i(\mathbf{e})}{\partial \mathbf{e}}\right]. \tag{4}$$

Finally, using quadratic energy functions, the constitutive problem in its incremental form can be put, as shown in the eq. (5), where $\mathbf{I}$ is the second order identity tensor. In addition, Θ and $\mathbf{F}$, corresponds, respectively, to the trace of the infinitesimal strain tensor and the gradient deformation tensor.

$$\begin{array}{c} \text{given,} \quad \Omega = \left\{[\mathbf{Q}_i]_n, \mathbf{F}_\mathrm{n}, \mathbf{F}_{\mathrm{n}+1}\right\}, \\ \text{compute:} \end{array} \begin{cases} \boldsymbol{\sigma}_{\mathrm{n}+1} = \mathrm{K}_\infty \Theta_{\mathrm{n}+1}\mathbf{I} + 2\mathrm{G}_\infty \mathbf{e}_{\mathrm{n}+1} + \sum_{i=1}^{k} 2\mathrm{G}_i \mathbf{e}_{n+1} - \sum_{i=1}^{k} [\mathbf{Q}_i]_{n+1} \\ [\mathbf{Q}_i]_{n+1} \quad \text{according to eq. (6)} \end{cases}. \tag{5}$$

$$[\mathbf{Q}_i]_{n+1} = \left(\frac{\tau_i}{1+\tau_i/\Delta t}\right)\left[\frac{1}{\tau_i}\left(2\mathrm{G}_i \mathbf{e}_{n+1}\right) + \frac{1}{\Delta t}[\mathbf{Q}_i]_n\right]. \tag{6}$$

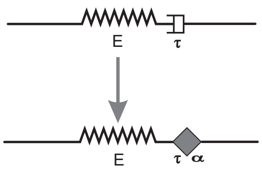

Figure 1. One-dimensional classical and fractional Maxwell's device

2.1 Fractional Models

The fractional models studied here are similar to the classic one shown above. The only difference relies on the evolution of internal variables that now is given by a fractional differential equation. The fractional model consists of replacing the dashpot by an element that allows the continuous transition between the viscous and elastic behavior, as can be shown in the one-dimensional rheological model presented in Fig. (1), where α is a new material parameter. This element recovers the elastic and viscous behavior for $\alpha = 0$ and $\alpha = 1$, respectively (Haveroth [10]).

As previous mentioned, in this work the Grünwald-Letnikov (G.L) definition is used. This definition is given by the limit of a sum and can be obtained by generalizing the integer order derivative, as shown in the eq. (7) for a differentiable function, $f(t)$. Where, Γ and Δt, are the Gamma function and the time step. The derivation steps are presented in detail in Oldham and Spanier [11].

$$\frac{d^\alpha}{dt^\alpha} f(t) = \lim_{N\to\infty} \left\{ \frac{[\Delta t]^{-\alpha}}{\Gamma(-\alpha)} \sum_{j=0}^{N-1} \frac{\Gamma(j-\alpha)}{\Gamma(j+1)} f(t - j\Delta t) \right\}. \tag{7}$$

The fractional viscoelastic model based on internal variables is given by a fractional differential equation, as presented in the eq. (8). This format was proposed by Adolfsson and Enelund [6], where the finite kinematics has been constrained to infinitesimal kinematics in the present work.

$$\frac{d^\alpha \mathbf{Q}_i}{dt^\alpha} + \frac{\mathbf{Q}_i}{\tau_i^\alpha} = \frac{1}{\tau_i^\alpha} \mathrm{dev}\left[\frac{\partial \Psi_i(\mathbf{e})}{\partial \mathbf{e}}\right]. \tag{8}$$

The total stress given by the eq. (3) remains identical for the fractional model. Using the G.L fractional derivative we can obtain the discrete form of the internal variable equation, as shown in eq. (9).

$$[\mathbf{Q}_i]_{n+1} = \left(\frac{\tau_i^\alpha}{1 + \tau_i^\alpha/\Delta t}\right) \left[\frac{1}{\tau_i^\alpha}\left(2\mathrm{G}_i \mathbf{e}_{n+1}\right) - \frac{1}{\Delta t^\alpha} \sum_{j=1}^{N-1} A_{j+1} \mathbf{Q}_i(t_{\mathrm{n}+1} - j\Delta t_{\mathrm{n}})\right]. \tag{9}$$

Comparing the fractional eq. (9) with the classical eq. (6), we can observe that the fractional model recovers the classical for $\alpha = 1$, since $\mathrm{A}_2 = -1$ and $\mathrm{A}_3 = \mathrm{A}_4 = \mathrm{A}_\mathrm{N} = 0$. Finally, the incremental fractional constitutive problem with infinitesimal kinematics can be defined as,

$$\begin{array}{ll} \text{given,} \quad \Omega = \left\{[\mathbf{Q}_i]_n, \mathbf{F}_\mathrm{n}, \mathbf{F}_{\mathrm{n}+1}\right\}, & \begin{cases} \boldsymbol{\sigma}_{\mathrm{n}+1} = \mathrm{K}_\infty \Theta_{\mathrm{n}+1}\mathbf{I} + 2\mathrm{G}_\infty \mathbf{e}_{\mathrm{n}+1} + \sum_{i=1}^{k} 2\mathrm{G}_i \mathbf{e}_{\mathrm{n}+1} - \sum_{i=1}^{k} [\mathbf{Q}_i]_{n+1} \\ [\mathbf{Q}_i]_{n+1} \quad \text{According to the eq. (9).} \end{cases} \\ \text{compute:} & \end{array}. \tag{10}$$

The classical and fractional models with finite kinematics were formulated in a similar way to the infinitesimal ones, only performing the proper kinematics considerations, as presented in Adolfsson and Enelund [6], Simo and Hughes [8].

3 Results

The research group carried out cyclic and creep-recovery experimental tests, both on UHMWPE compression samples. The cyclic tests were performed at two different strain rates and the creep-recovery tests at two stress levels. Each test was repeated three times, using three different specimens, to ensure repeatability of results. The experimental results presented in Fig. 2 are shown in true strain and nominal stress (or engineering stress). The cyclic tests were performed at strain rates of 0.01% and 0.1% per second. The loading ramp was performed with displacement control. The maximum amount of deformation was defined as the instant when the applied compression load reached the nominal stress of 16 MPa. The motivation to control the maximum deformation by the load and not by the displacement, was due to the need to protect the load cell, which supported up to 500 N. Once this value was reached, the unloading ramp started at the same rate as the load. The minimum deformation value was set to the instant when the load reached 2 N. This decision was taken to ensure contact between the compression device and the sample.

The creep-recovery tests were conducted at two stress levels, 4 and 8 MPa. The loading ramp was performed at a rate of 2 MPa/min until the test stress was reached. The samples were then held in creep for 24 hours. At the end of this period they were unloaded up to the value of 2 N (for the same reason cited in the cyclic test). After reaching this value the samples were kept in recovery for another 24h under load control.

3.1 Experimental curve fitting

As previously mentioned, this work seeks to compare the results of parameter fitting between classic and fractional viscoelastic models. To complete this objective, curves were fitted in cyclic and creep-recovery loading. First the experimental data are fitted separately. Then the results are presented using two creep and two cyclic curves simultaneously. The simultaneous fitting is interesting because it allows to obtain a set of parameters able to simulate the material behavior in various loading conditions. As pointed before, we investigated whether fractional models improve the fitting ability using various experimental data. It is important to emphasize the use in the literature of elasto-viscoplastic or viscoelastic-viscoplastic models for modeling the UHMWPE (Avanzini [12], Bergström et al. [13, 14], Chen et al. [15], Hassan et al. [16], Khan et al. [17]). However, viscoelastic models are used in this work in order to verify the adequacy and possible improvement when using fractional models. The Table 1 shows the correspondence between the model names and the abbreviations used in this results section. The number of branches corresponds to the number of Maxwell's devices used .

Table 1. Abbreviation of model names used throughout the text.

	Classic Viscoelastic Models (CVE)				Fractional Viscoelastic Models (FVE)			
Kinematics	Infinitesimal (IN)		Finite (FN)		Infinitesimal (IN)		Finite (FN)	
Branches	1	2	1	2	1	2	1	2
Abbreviations	CVE-IN-1	CVE-IN-2	CVE-FN-1	CVE-FN-2	FVE-IN-1	FVE-IN-2	FVE-FN-1	FVE-FN-2

Figures 2 and 3 show the results using one and two viscoelastic branches, respectively, in creep-recovery and cyclic loading. It can be observed that using only one branch, the fractional models allows smoother curves compared to the classic ones, including in the recovery phase. Whereas using two branches, the two model classes showed very similar results. Curiously, the derivative orders of the fractional models converge to 1, that is, to the classic models. Although viscoelastic models have represented the qualitative cyclic behaviour, the shapes of the numerical curves are not in accordance with the experimental data, mainly in the loading phase. This fact may be related to the existence of other nonlinear phenomena not taken into account, such as ratchetting (Chen et al. [15] and Yu et al. [18]). To help the comparison, Table 2 presents a rank containing the number of parameters and values of the objective function, $g(\mathbf{x})$, obtained in the fittings using cyclic and creep-recovery data separately.

Table 2. Rank with information of number of parameters and value of the objective function. Creep and Cyclical data fitted separately.

Model	CVE-FN-2	FVE-FN-2	CVE-IN-2	FVE-IN-2	FVE-FN-1	FVE-IN-1	CVE-FN-1	CVE-IN-1
Number of parameters	5	7	5	7	4	4	3	3
$g(\boldsymbol{x})[10^3]$-Creep-recovery	6.01	6.03	7.32	7.32	7.77	8.98	10.66	11.88
$g(\boldsymbol{x})[10^2]$-Cyclic	3.61	3.61	2.72	2.72	4.59	3.54	8.11	6.64

It is also interesting to analyze the processing time spent on solving the optimization problem. Table 3 shows the CPU time for the fitting using two viscoelastic branches with infinitesimal and finite kinematics. The results refer to the complete optimization process, i.e., five rounds of PSO are performed, followed by the gradient-based method. The data were normalized in relation to the time spent by the classic two branches model (CVE-IN-2). As it can be seen, the fractional models had a computational cost considerably higher than the classics, reaching

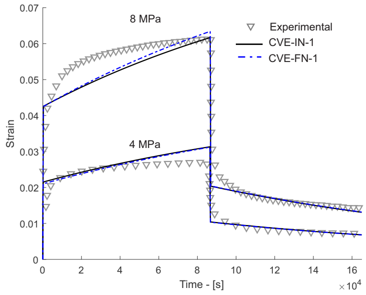

(a) Classic models - One branch

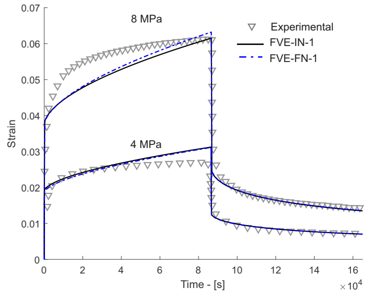

(b) Fractional models - One branch

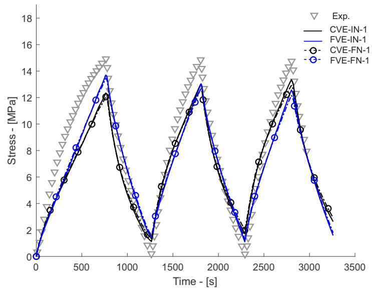

(c) Strain rate of $0.01\%s^{-1}$ - One branch

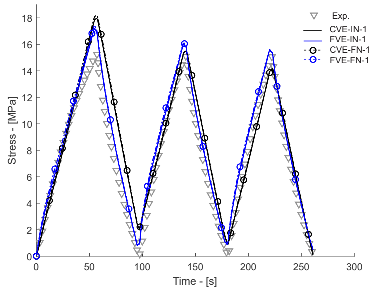

(d) Strain rate of $0.1\%s^{-1}$ - One branch

Figure 2. Experimental and numerical data in creep-recovery and cyclic loading. Parameter fitting using data separately and one viscoelastic Maxwell's device.

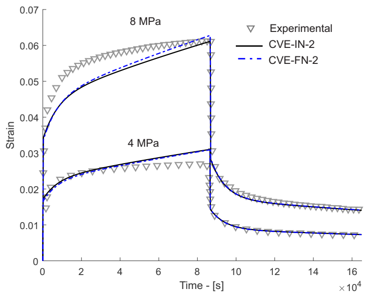

(a) Classic - Two branches

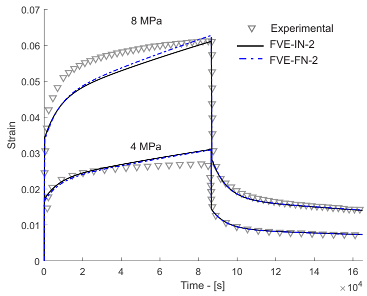

(b) Fractional models - Two branches

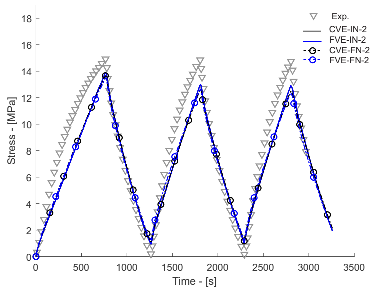

(c) Strain rate of $0.01\%s^{-1}$ - Two branches

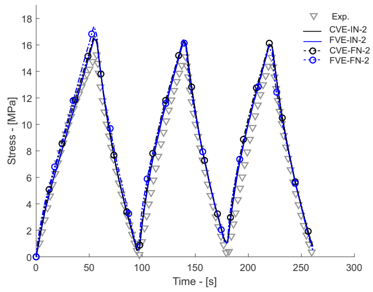

(d) Strain rate of $0.1\%s^{-1}$ - Two branches

Figure 3. Experimental and numerical data in creep-recovery and cyclic loading. Parameter fitting using data separately and two viscoelastic Maxwell's devices.

Table 3. CPU time to solve the optimization for the models with two branches.

Models	CVE-IN-2	FVE-IN-2	CVE-FN-2	FVE-FN-2
Relative time [s/s]	1	2.86 times CVE-IN-2	3.04 times CVE-IN-2	4.57 times CVE-IN-2

times even 4.5x greater than the CVE-IN-2. This is related to the fact that the fractional models consider all the past history of the internal variables. It is important to mention that some authors present techniques to reduce this cost, such as Schmidt and Gaul [19] and Zopf et al. [20]. In this work we have not used such techniques, because the objective is to analyze the possible improvement when using fractional models and compare them with the classics.

From this point on we will present the results using simultaneously cyclical and creep data for parameter fitting. Table 4 shows the parameters and values of the objective function, $g(\mathbf{x})$, using one and two branches. From Table 4 one can see that the fractional models presented better objective function results, including when it is used two branches. The difference between the classic and fractional models with one branch is considerably large. While with two this difference is smaller.

While for the individual fittings the fractional model converged to the classic one, in the simultaneous fitting this does not happen. We can see that one of derivative orders (α) found was not integer, as shown in Table 4. In general, it can be said that the fractional models have slightly improved the simultaneous fittings.

Table 4. Viscoelastic parameters in creep-recovery and cyclic loading with infinitesimal and finite strain. Sorted according to the value of the objective function.

	$g(\boldsymbol{x})[10^{-2}]$			ν_0	G_∞	G_1	$\tau_1[10^3]$	α_1	G_2	τ_2	α_2
Models	Total	Cyclic	Creep								
FVE-IN-2	5.66	4.13	1.52	0.46	10.00	34.7765	251.7401	1	147.4471	46.8032	0.7312
FVE-FN-2	6.40	4.94	1.46	0.46	3.6895	43.3337	303.8491	0.9999	167.6226	39.5119	0.7108
CVE-IN-2	6.62	5.38	1.24	0.46	17.2565	30.4868	170.7551	-	113.5487	85.6239	-
CVE-FN-2	7.57	6.45	1.12	0.46	17.4256	33.2461	168.0647	-	122.1393	82.5703	-
FVE-IN-1	12.01	5.46	6.54	0.46	17.7980	35820.6522	1.6539×10^{-12}	0.2456	-	-	-
FVE-FN-1	13.05	6.38	6.66	0.46	18.3599	37229.2685	1.6881×10^{-12}	0.2446	-	-	-
CVE-IN-1	28.24	5.024	23.22	0.46	44.1903	115.2043	93.4580×10^{-3}	-	-	-	-
CVE-FN-1	29.35	6.11	23.24	0.46	46.6825	123.7070	91.0634×10^{-3}	-	-	-	-

4 Conclusions

As presented, the main objective of this work was the comparison between classic and fractional viscoelastic models using experimental data from the UHMWPE under cyclic and creep-recovery loading. The experimental results under these conditions were shown and fittings were made using a hybrid optimization procedure. In the individuals fittings the fractional models showed better performance when only one viscoelastic branch was used. However, this improvement became insignificant with two or more branches. Whereas in the simultaneous fitting, the fractional models were superior to the classics using one and two viscoelastic Maxwell's devices. However, this improvement was small with two branches. In addition, it should also be considered that fractional models require higher computational cost than classic models, since it considers the complete history of internal variables (or a portion, when cost reduction techniques are used). In this way, the use of classic models can be more interesting, since they present similar results as fractional models when, at least, two branches are used. Comparing the models with infinitesimal and finite kinematics, we show that the use of the second class did not result in significant improvement. This may justify the choice for models with infinitesimal kinematics and indicates that material nonlinearity may be predominant in relation to geometry nonlinearity, under these presented test conditions. Finally, it was observed that the numerical results in creep-recovery showed better agreement with the experimental data, while the shape of predicted cyclic tests were not represented satisfactorily. This may be related to nonlinear phenomena not taken into account in the presented viscoelastic models, such as ratcheting. Therefore, it is suggested the formulation of viscoelastic-viscoplastic models capable of representing the shape of the curve in the loading phase in cyclical tests. In a next work we will present this class of models with classic and fractional formulations.

Acknowledgements. Financial supports by the Brazilian agencies CAPES and CNPq, are appreciated.

Authorship statement. The authors hereby confirm that they are the sole liable persons responsible for the authorship of this work, and that all material that has been herein included as part of the present paper is either the property (and authorship) of the authors, or has the permission of the owners to be included here.

References

[1] Ward, I. M. & Sweeney, J., 2012. *Mechanical properties of solid polymers*. John Wiley & Sons.
[2] Xu, J., Chen, Y., Tai, Y., Xu, X., Shi, G., & Chen, N., 2020. Vibration analysis of complex fractional viscoelastic beam structures by the wave method. *International Journal of Mechanical Sciences*, vol. 167, pp. 105204.
[3] Amabili, M., Balasubramanian, P., & Breslavsky, I., 2019. Anisotropic fractional viscoelastic constitutive models for human descending thoracic aortas. *Journal of the mechanical behavior of biomedical materials*, vol. 99, pp. 186–197.
[4] Meng, R., Yin, D., & Drapaca, C. S., 2019. A variable order fractional constitutive model of the viscoelastic behavior of polymers. *International Journal of Non-Linear Mechanics*, vol. 113, pp. 171–177.
[5] Xiao, R., Sun, H., & Chen, W., 2016. An equivalence between generalized Maxwell model and fractional Zener model. *Mechanics of Materials*, vol. 100, pp. 148–153.
[6] Adolfsson, K. & Enelund, M., 2003. Fractional derivative viscoelasticity at large deformations. *Nonlinear dynamics*, vol. 33, n. 3, pp. 301–321.
[7] Khajehsaeid, H., 2018. Application of fractional time derivatives in modeling the finite deformation viscoelastic behavior of carbon-black filled nr and sbr. *Polymer Testing*, vol. 68, pp. 110–115.
[8] Simo, J. C. & Hughes, T. J., 2006. *Computational inelasticity*, volume 7. Springer Science & Business Media.
[9] Tschoegl, N. W., Knauss, W. G., & Emri, I., 2002. Poisson's ratio in linear viscoelasticity–a critical review. *Mechanics of Time-Dependent Materials*, vol. 6, n. 1, pp. 3–51.
[10] Haveroth, T. C. d. C., 2015. On the use of fractional derivatives for modeling nonlinear viscoelasticity.
[11] Oldham, K. & Spanier, J., 2002. *The fractional calculus theory and applications of differentiation and integration to arbitrary order*, volume 111. Elsevier.
[12] Avanzini, A., 2008. Mechanical characterization and finite element modelling of cyclic stress–strain behaviour of ultra high molecular weight polyethylene. *Materials & Design*, vol. 29, n. 2, pp. 330–343.
[13] Bergström, J., Kurtz, S., Rimnac, C., & Edidin, A., 2002. Constitutive modeling of ultra-high molecular weight polyethylene under large-deformation and cyclic loading conditions. *Biomaterials*, vol. 23, n. 11, pp. 2329–2343.
[14] Bergström, J., Rimnac, C., & Kurtz, S., 2004. An augmented hybrid constitutive model for simulation of unloading and cyclic loading behavior of conventional and highly crosslinked uhmwpe. *Biomaterials*, vol. 25, n. 11, pp. 2171–2178.
[15] Chen, K., Kang, G., Yu, C., Lu, F., & Jiang, H., 2016. Time-dependent uniaxial ratchetting of ultrahigh molecular weight polyethylene polymer: viscoelastic–viscoplastic constitutive model. *Journal of Applied Mechanics*, vol. 83, n. 10.
[16] Hassan, T., Çolak, O. U., & Clayton, P. M., 2011. Uniaxial strain and stress-controlled cyclic responses of ultrahigh molecular weight polyethylene: experiments and model simulations. *Journal of engineering materials and technology*, vol. 133, n. 2.
[17] Khan, F., Yeakle, C., & Gomaa, S., 2012. Characterization of the mechanical properties of a new grade of ultra high molecular weight polyethylene and modeling with the viscoplasticity based on overstress. *Journal of the mechanical behavior of biomedical materials*, vol. 6, pp. 174–180.
[18] Yu, C., Kang, G., Chen, K., & Lu, F., 2017. A thermo-mechanically coupled nonlinear viscoelastic–viscoplastic cyclic constitutive model for polymeric materials. *Mechanics of Materials*, vol. 105, pp. 1–15.
[19] Schmidt, A. & Gaul, L., 2002. Application of fractional calculus to viscoelastically damped structures in the finite element method. In *Proceedings of the International Conference on Structural Dynamics Modelling*, pp. 297–306.
[20] Zopf, C., Hoque, S., & Kaliske, M., 2015. Comparison of approaches to model viscoelasticity based on fractional time derivatives. *Computational Materials Science*, vol. 98, pp. 287–296.